Trenchless Technology Center
Louisiana Tech University

2012

Experimental Evaluation of Selected Limit States of Aqua-Pipe® Liner at Locations of Ring Fracture

Prepared for:
Ben Cote, Vice President
Sanexen Environmental Services Inc.
1471 Lionel-Boulet Blvd., Ste. 32
Varennes, QC J3X 1P7
Canada

Prepared by:
Erez N. Allouche, PhD, P.Eng.
Shaurav Alam, Ph.D.

April 11, 2012

Executive Summary

This report presents findings of an 18-month long experimental study by the Trenchless Technology Center (TTC) on the performance of Aqua-Pipe® liner at locations of ring fracture, a prevalent mode of failure in small diameter cast iron water mains. The study was undertaken due to the fact that differential ground movements induced by frost, moisture changes in 'reactive' clays, or a nearby excavation, could cause the loss of 'beam support' at the pipe's invert, and a subsequent formation of a transverse (or 'ring') fracture in the brittle cast iron pipe. Differential vertical, lateral, and/or axial movement of the host pipe at the location of the ring fracture, as a result of internal water pressure and/or uneven ground movement can induce loading mechanisms commonly not considered in the design of such liners, which in return may lead to liner instability.

The work reported herein investigates three limit states, namely flexure, shear, and axial loading conditions. Six specimens, each comprised of two 4 ft. long sections of a 70 year old 6 in. cast iron pipe, were prepared by forming a simulated transverse ring break at their lengthwise middle point. The specimens were then lined with an Aqua-Pipe® liner. Tests were performed for both pressurized and non-pressurized conditions. For the case of testing under pressurized conditions, the specimens were capped and subjected to three-point bending, uni-axial tensile, and shear loads using custom-built testing apparatuses. In the non-pressurized condition tests, similar steps were followed, except that the end caps used were daunt shape, allowing access to the inner surface of the liner.

The behaviors of the host pipe and the liner were monitored with an increased level of applied load, and geometrical changes in the liners were noted. Strain measurements in the axial and hoop directions within the liner at the location of the ring fracture were also monitored. A numerical study was performed on the bending behavior of the liner. Observations are reported regarding governing failure mechanisms for an Aqua-Pipe® liner subjected to bending, shear, or uni-axial displacements at the location of ring fracture.

TABLE OF CONTENTS

Executive Summary 2
Tables 4
Figures 5
1. INTRODUCTION 7
2. PREPARATION OF SAMPLE 8
3. BENDING TEST 10
3.1. PRESSURIZED CONDITION 10
3.2. NON-PRESSURIZED CONDITION 12
4. TENSILE TEST 16
4.1. NON-PRESSURIZED CONDITION 16
5. SHEAR TEST 17
5.1. PRESSURIZED CONDITION 17
5.2. NON-PRESSURIZED CONDITION 18
6. CONCLUSION 21
7. REFERENCES 22

TABLES

Table 1: Geometrical changes at the pipe-liner interface with increased vertical deflection under pressurized condition..... 11
Table 2: Identification of strain gages and strain rosettes connections 13
Table 3: Reading recorded during the non-pressurized bending test..... 15

FIGURES

Figure 1: Forces resulted from bending and shear movement of the host-pipe 7
Figure 2: Forces resulted from tensile movement of the host-pipe 7
Figure 3: Location of wooden spacer (left) and wooden spacer in between the host-pipe sections (left) 8
Figure 4: Specimens after lining (left); host-pipe sections after removal of clamps and spacer (right) 8
Figure 5: Solid cap with pressure gauge (left) and hollow cap (right) 9
Figure 6: Test specimen hung over the cap (left), application of polyurea (middle) and final setup (right) 9
Figure 7: Pressurized leak test performed on the test specimen 9
Figure 8: Host pipe placed on custom built support (left) and deflection measurements (right) 10
Figure 9: Pressure gauge (left) and manually operated pressure pump with pressure regulator (right) 10
Figure 10: Resin started cracking (left) and host pipe cracked parallel to spring line (right) 12
Figure 11: Crushed host-pipe (left); deflected liner holding120 psi internal pressure (middle); deformation at the liner's crown region (right) 12
Figure 12: Placement (left) and arrangements of strain gages (middle) and strain rosettes (right) 13
Figure 13: Location of strain gauges and strain rosettes on inner liner wall 13
Figure 14: Different stages in the formation of a fold at the invert of the liner 14
Figure 15: Response of strain rosettes at spring-line (left) and strain gauge at invert (right) 14
Figure 16: Specimen been restraint at one end (left) and been pulled at other end (right) 16
Figure 17: Pulling force vs. displacement 16
Figure 18: Experimental setup of the shear test (left) and the nitrogen gas operated pressure pump (right) 17
Figure 19: Response of strain rosettes at crown (left) and spring-line (at location of externally applied load; right) 18

Figure 20: Host-pipe broke at crown-invert plane (left) and 3.5 in. displacement of the liner (right) 18
Figure 21: Schematic diagram of test specimen 19
Figure 22: Strain gauge installed on the liner 19
Figure 23: Response of strain rosettes at spring-line (west) (left) and at invert (right) 20
Figure 24: Response of strain rosettes at spring-line (west) (left) and at invert (right) 20
Figure 25: Formation of fold at the invert due to vertical displacement (left); lateral deformation of the liner caused by lateral displacement (right) 21

1. INTRODUCTION

Structural liners meeting the standards ASTM F1743 and ASTM F1216 are designed for a service life of around 50 years. During this long service life, liners withstand various types of external loads, e.g., flexure, shear, and tensile, in addition to the internal operating pressure. Moreover, a sudden change in the loading condition on the liner (i.e., a singularity within the host pipe continuum) may arise when the host-pipe breaks or shifts as a result of uneven ground movement, thus creating concentrated stresses at these locations.

This experimental research focuses on the behavior of the Aqua-Pipe® Liner subjected to bending, shear, and tension under both pressurized and non-pressurized conditions at the location of the ring fracture. Figure 1 and Figure 2 shows the qualitative consequence of flexure, shear, and tensile forces on the liner caused by differential movement of the host pipe at the location of the ring fracture.

Figure 1: Forces resulted from bending and shear movement of the host-pipe

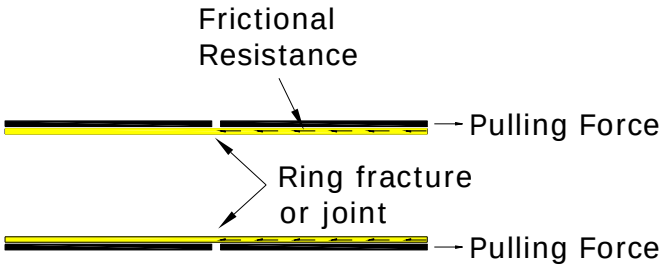

Figure 2: Forces resulted from tensile movement of the host-pipe

2. PREPARATION OF SAMPLE

Test specimens were prepared using 6 in. diameter, 4 ft. long cast iron host-pipes, which were in service for 70 years. The uneven internal surface of the host pipe supported mechanical interlock between the resin and the host pipe. First, the host-pipe was cut into two halves and a thin circular wooden spacer was placed between them. Next, a mechanical clamp was used to hold the sections contiguously and the samples were sent to Montreal, Canada, to be lined (see Figure 3). The lined specimens were shipped back to the Trenchless Technology Center, where the wooden spacer was removed to form the simulated ring fracture between the host-pipe sections (see Figure 4).

Figure 3: Location of wooden spacer (left) and wooden spacer in between the host-pipe sections (left)

Figure 4: Specimens after lining (left); host-pipe sections after removal of clamps and spacer (right)

Two main categories of tests were performed: pressurized condition and non-pressurized condition. For the pressurized tests, the samples were capped on both edges using two solid circular covers, and pressurized internally with water using a high pressure manually operated pump. Caps were built out of two 6 in. circular steel sections (one 8 in.dia. and the other 5 in. dia.) welded concentrically on an 8 in. dia. circular plate. Quick-connectors and valves were attached to the cap to facilitate flow of water in and out of the test specimen and to apply pressure internally on the liner. For the non-pressurized condition test, caps were built following a similar procedure, except the cap was made hollow by welding a donut shaped end circular plate. Strain gauges and strain rosettes were installed on the liner to obtain real-time strain and stress measurements (see Figure 5).

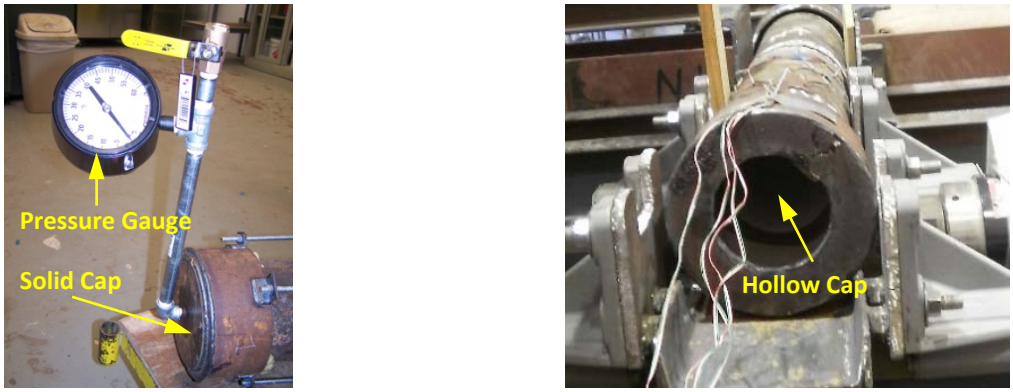

Figure 5: Solid cap with pressure gauge (left) and hollow cap (right)

The annulus between the caps and the specimen's wall was sealed using polyurea (Part A + B organic compound with rapid setting time), making the specimens leak proof (see Figure 6).

Figure 6: Test specimen hung over the cap (left), application of polyurea (middle) and final setup (right)

A leak test was performed using a high pressure pump to test the polyurea seal prior to commencement of the actual test. The pressure was held at 20 psi for about 30 minutes to confirm a tight seal at the edges of the capped specimen (see Figure 7).

Figure 7: Pressurized leak test performed on the test specimen

3. BENDING TEST

The capped test specimen was placed on two custom built supports for the bending test. Wooden planks were used to restrict the rotation of the test specimen about its neutral axis. A digital spirit level was attached at the crown of the host-pipe to measure angular displacement of the specimen throughout the test. As the host pipe was noncontiguous at its center, a hinge condition was developed at that location of the pipe under the applied external load as shown in Figure 8.

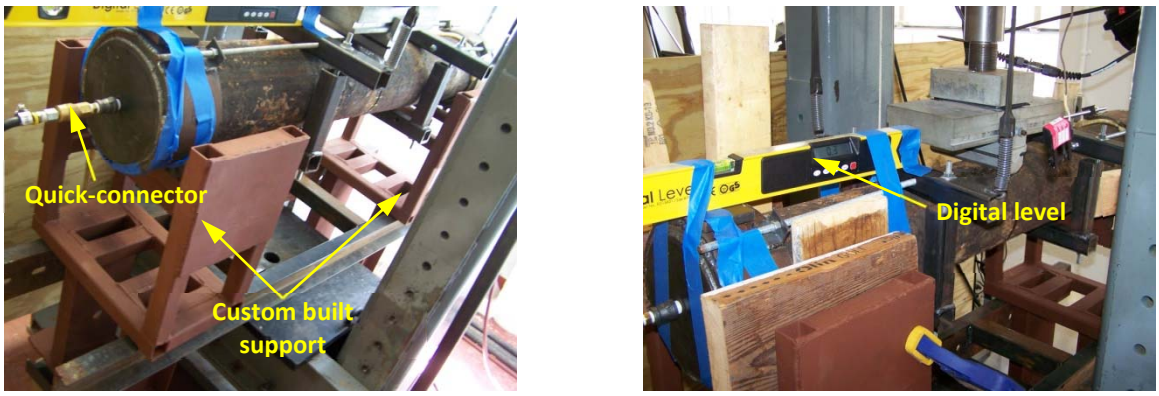

Figure 8: Host pipe placed on custom built support (left) and deflection measurements (right)

3.1. PRESSURIZED CONDITION

During the pressurized experiment, the internal pressure within the specimen was monitored at all times using a pressure gauge. A pressure regulator was used to restrict the applied internal pressure to a maximum of 120 psi (see Figure 9). A 50 kip MTS servo-controlled actuator was used to apply a point load to the location of the ring fracture (3-polint load loading configuration), resulting in a vertical deflection at the invert of the cast iron host pipe to increase 0 in. to approximately 5 in. in increments of 0.25 in., corresponding to an angular displacement of about 12.5°. The angular displacement was read using the digital level. Table 1 provides a summary of the geometrical changes observed for the host pipe and liner with an increased vertical deflection.

Figure 9: Pressure gauge (left) and manually operated pressure pump with pressure regulator (right)

Table 1: Geometrical changes at the pipe-liner interface with increased vertical deflection under pressurized condition

Reading No.	Displacement		Internal Pressure	Gap Between Host-pipe and Liner					Load	Comments
				Spring-line			Invert			
	V	A		1	2	3	H	V		
	in	°	psi	in	in	in	in	in	Kip	
1	0	0	5	0.25	0.24	0.23	0	0	0.00	
2	0.25	0	5	0.25	0.22	0.23	0	0	0.50	
3	0.50	0.1	5	0.25	0.22	0.24	0.05	0	2.73	
4	0.76	0.3	5	0.29	0.27	0.30	0.19	0.02	4.30	
5	1.00	0.8	5	0.35	0.36	0.40	0.49	0.09	5.15	
6	1.25	1.3	5	0.42	0.45	0.48	0.68	0.15	5.69	
7	1.50	1.9	5	0.49	0.52	0.62	0.82	0.19	6.24	
8	1.75	2.7	5	0.58	0.63	0.68	0.96	0.24	6.85	
9	2.00	3.4	5	0.67	0.74	0.82	1.10	0.24	7.10	
	2.00	3.5	20	0.65	0.71	0.81	1.08	0.22		
10	2.25	4.1	5	0.76	0.84	0.94	1.20	0.25	7.65	
11	2.50	5.8	5	0.94	1.10	1.20	1.96	0.32	8.02	
12	2.75	6.5	5	1.00	1.15	1.33	1.76	0.37	7.79	Crack in the pipe at crown
	2.75	6.8	30	1.00	1.15	1.33	1.75	0.36		
13	3.00	7.4	30	1.10	1.27	1.41	1.93	0.38	8.13	
14	3.25	8.2	60	1.20	1.39	1.62	2.07	0.42	8.12	Adhesion broke
15	3.50	8.9	60	1.26	1.48	1.73	2.20	0.47	8.35	
16	3.75	9.6	60	1.28	1.50	1.75	2.27	0.52	8.55	Pipe cracked parallel to SL
17	4.00	10.3	60	1.24	1.46	1.68	1.59	0.55	9.40	
18	4.50	11.1	60	1.29	1.54	1.73	2.39	0.65	9.70	Host-pipe crushed
19	5.00	12.8	120	1.25	1.55	1.72	2.38	0.67	10.22	

The internal pressure was kept at 5 psi until vertical displacement reached 2 in.. At this point, internal pressure was increased to 20 psi; the gap between the host pipe and liner was reduced due to the increase in pressure. The internal pressure was reduced again to 5 psi and the vertical displacement was increased to 2.25 in.; at this point, the host-pipe cracked at the crown. The cycle of increasing the vertical displacement by 0.25 in., followed by pressurizing the specimen to 30 psi, continued until vertical displacement reached 3.0 in.. At a vertical displacement of 3.25 in., the internal pressure was increased to 60 psi. The host pipe cracked at the spring line at a vertical displacement of 3.7 in., resulting in relaxation of the adhesion between the host pipe and the liner at the vicinity of the circumferential crack (see Figure 10).

Figure 10: Resin started cracking (left) and host pipe cracked parallel to spring line (right)

At a vertical displacement of 4.0 in. with 60 psi internal pressure, the liner began to protrude. The host-pipe crushed at a vertical displacement of 4.5 in; however, at a vertical displacement of 5 in., the liner was still holding 120 psi with no visible sign of failure of the liner. The test was terminated at this point and the liner was removed from the host pipe. An image of the liner following the test is given in Figure 11. The host-pipe cracked and the liner deformed at the crown at the location of the externally applied load.

Figure 11: Crushed host-pipe (left); deflected liner holding120 psi internal pressure (middle); deformation at the liner's crown region (right)

3.2. NON-PRESSURIZED CONDITION

In the non-pressurized condition test, both ends of the test specimen were capped using hollow caps. Strain gauges and rosettes were installed inside the liner along the longitudinal axis, in the proximity of the simulated fracture location, to measure strain levels. As the loading condition was a simply supported beam subject to a point load at its center point, tensile and compressive stress zones developed below and above the plane of the longitudinal neutral axis, respectively. Two strain gauges were installed parallel to the direction of the longitudinal neutral plane on the crown and invert of the inner surface of the liner. Hoop stresses were expected along the circumference, so two strain rosettes were installed on the spring-line plane. Layout and location of the strain gauges and strain rosettes are shown in Figure 12 and Figure 13, respectively. The locations were marked and later named after the respective connection port in the data acquisition system (see Table 2).

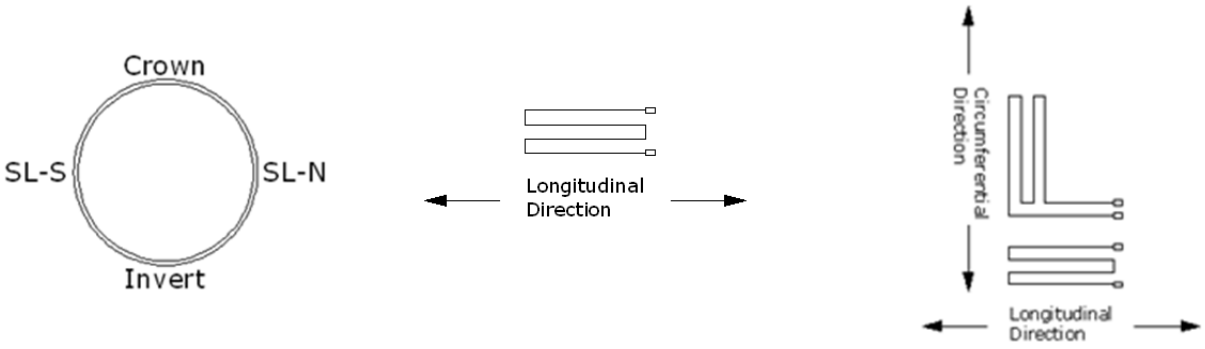

Figure 12: Placement (left) and arrangements of strain gages (middle) and strain rosettes (right)

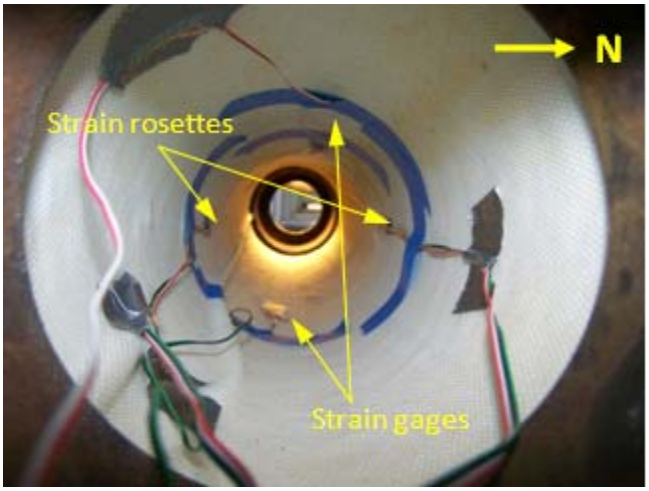

Figure 13: Location of strain gauges and strain rosettes on inner liner wall

Table 2: Identification of strain gages and strain rosettes connections

SL. No.	Type	Direction	Location	Connection on Data Module	Name
1	Strain rosettes	Longitudinal	Spring line - North	101	SR-long-SLN-101
2	Strain rosettes	Circumferential	Spring line – North	102	SR-Cir-SLN-102
3	Strain gage	Longitudinal	Invert	103	SG-long-I-103
4	Strain rosettes	Longitudinal	Spring line – South	104	SR-long-SLS-104
5	Strain rosettes	Circumferential	Spring line – South	105	SR-Cir-SLS-105
6	Strain gage	Longitudinal	Crown	106	SG-long-C-106

After the testing setup was completed, a 50 kip capacity servo-control actuator was used to apply the external load to the specimen to achieve pre-determined vertical displacement increments. As the internal pressure was zero, the liner deformed under the externally applied load. No vertical gaps were visible between the liner and the host pipe at the location of the ring break until the vertical displacement reached 1.75 in. At a vertical displacement of 3.25 in., the excess resin at

the ring break location cracked. As hoop stresses in the circumferential direction and tensile stresses in the longitudinal direction (at the invert) developed, the liner began to de-bond from the host-pipe at the invert, resulting in the formation of a fold at a vertical displacement of 3.50 in. At a vertical displacement of 4 in. (angular displacement near the center of the pipe ~14°), the fold formation at the invert reached 'maturity', indicating the on-set a buckling failure. The liner lost its structural integrity shortly after the formation of the fold (see Figure 14).

Figure 14: Different stages in the formation of a fold at the invert of the liner

Figure 15 displays the response of one of the strain rosettes and the strain gauge installed at the spring line and invert, respectively. As the ring fracture acted as a hinge connection under the applied vertical load, the liner below the neutral axis in the tensile zone displaced downward and elongated. On the spring-line and invert, no stress was produced until the crown deformed sufficiently to result in the formation of significant bending forces. At a vertical displacement of about 3.5 in, bond failure took place at the liner host-pipe interface and the transfer of all stresses to the liner (see the sudden increase in tensile stress and corresponding drop in hoop stress shown in Figure 15). The liner responded to this sudden increase in stress by undergoing a geometrical deformation (i.e., the formation of a fold), resulting in a gradual drop in the longitudinal stress at the invert and a corresponding increased in hoop stresses at the spring-line.

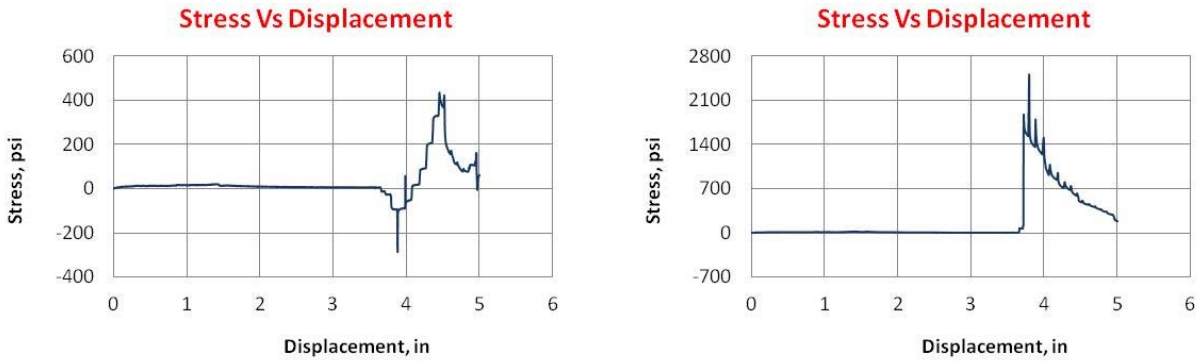

Figure 15: Response of strain rosettes at spring-line (left) and strain gauge at invert (right)

A summary of the experimental recorded data for the non-pressurized bending test, including vertical displacement and applied external force; the deflection angle and the gap between the host-pipe and the liner at the zone invert at the location of the ring fracture are given in Table 3.

Table 3: Reading recorded during the non-pressurized bending test

Sl. No.	Actual Displacement	Gap in Invert (in)			Load	Angle	Remarks
		Loc. 1	Loc. 2	Loc. 3			
	(in)	(in)	(in)	(in)	(lbf)	(deg)	
1	0.000	0.096	0.075	0.074	2.0	0.0	
2	0.250	0.159	0.155	0.134	97.0	0.0	
3	0.501	0.169	0.164	0.145	2091.0	0.1	
4	0.750	0.251	0.291	0.255	3568.0	0.5	
5	1.002	0.414	0.437	0.410	4846.0	1.2	
6	1.250	0.561	0.598	0.559	5562.0	1.9	
7	1.500	0.687	0.714	0.751	6491.0	2.7/2.8	Pipe starts twisting
8	1.750	0.838	0.881	0.905	6673.0	3.6	Annular gap starts
9	2.001	0.981	1.045	1.060	7281.0	4.4	
10	2.250	1.110	1.208	1.237	7508.0	5.2	
11	2.500	1.244	1.373	1.411	7573.0	6.0	
12	2.750	1.354	1.455	1.538	7912.0	6.8	
13	3.003	1.505	1.664	1.704	8035.0	7.5/7.6	
14	3.252	1.603	1.763	1.825	7850.0	8.3	Resin started breaking
15	3.502	1.711	1.859	1.900	7612.0	9.2	
16	3.750	1.827	1.982	2.100	7795.0	10.0	Liner started buckling
17	4.001	1.913	2.165	2.225	7884.0	10.9	Liner buckled on invert
18	4.502	2.203	2.416	2.498	8073.0	12.5	
19	5.000	2.434	2.768	2.890	6312.0	14.3	

4. TENSILE TEST

4.1. NON-PRESSURIZED CONDITION

The tensile uni-axial test was performed under non-pressurized conditions. One end of the capped specimen was held in place by a specially built frame, while the other end was connected to a 150,000 lb servo-control hydraulic actuator via a swivel connection. Two parabolic-shaped cut rods forming an umbrella skeleton were welded to each cap. Next, the actuator was pulled at a rate of 0.12 in/min until the host-pipe was observed slipping out of the liner at the location of the ring fracture. The average thickness of the pipe and the liner were measured to be 0.554 in. and 0.182 in., respectively. Based on a contact length of 48.0 in. and an outer diameter of 6.95-in., the total contact area between the liner and host-pipe were found to be 881 in^2. A pullout force of 11.5 kip (see Figure 17) was needed to overcome the friction between the liner and the host pipe (i.e., mobilize the liner), representing a friction value of approximately 13 psi (or 1800 lbf per square foot).

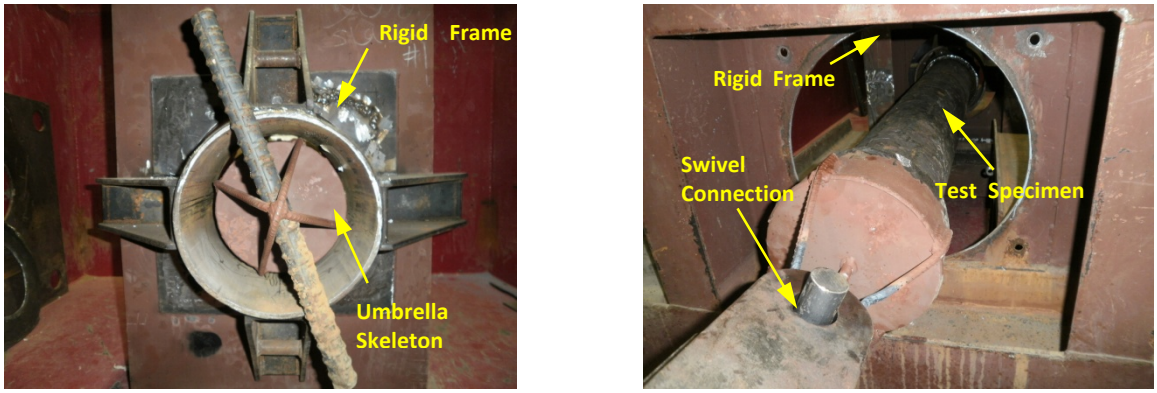

Figure 16: Specimen been restraint at one end (left) and been pulled at other end (right)

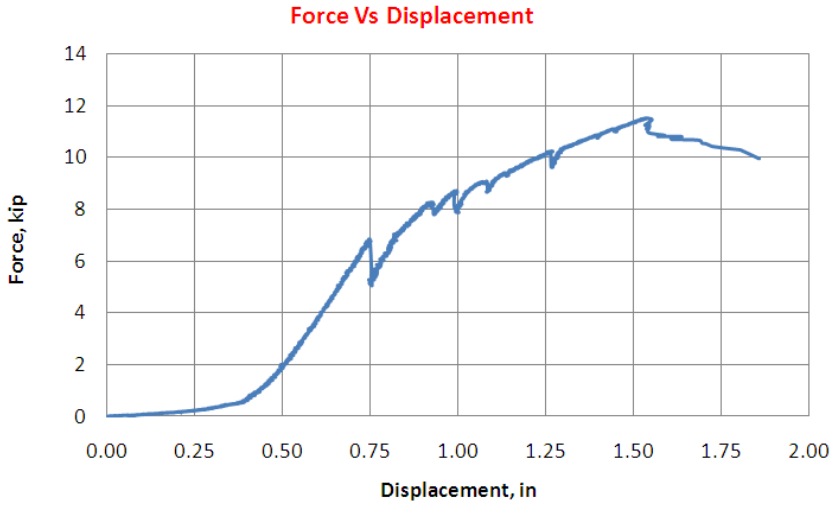

Figure 17: Pulling force vs. displacement

5. SHEAR TEST

A custom setup was designed and built to apply the shear load to the liner at the location of ring fracture. One half of the test specimen was restrained in all directions, while the other half was allowed to move only perpendicular to the longitudinal axis of the host-pipe. The restrained half was positioned inside two steel C-channels, ensuring complete rigidity. The other half was placed inside a steel box that was bolted onto four guiderails. The head of a 150 kip servo controlled hydraulic actuator was positioned such that no bending moment took place at the location of the simulated ring break.

5.1. PRESSURIZED CONDITION

For the pressurized condition test, the specimen was prepared following the same procedure as the flexure test specimen and placed carefully inside the test setup. A strip of orange paint was placed along the crown of the specimen to allow better visualization of the lateral movement across the ring fracture. A nitrogen gas operated pressure pump was used to generate internal pressure inside the pipe specimen (see Figure 18).

Figure 18: Experimental setup of the shear test (left) and the nitrogen gas operated pressure pump (right)

Strain rosettes placed at the liner's crown, invert, and spring-lines were used to record the resulting longitudinal and circumferential stresses induced by the shear displacement. The actuator was moved at increments of 0.25 in., while the pipe specimen was subjected to a pressure of 60 psi. Readings recorded by strain rosettes located at the crown and spring-line locations are shown in Figure 19. The longitudinal stress at the spring-line increased to around 3800 psi and the hoop stress was approximately 500 psi (compression). Similar peak stress values were recorded by the strain rosette located at the crown region. When the displacement reached 0.9 in., the host-pipe cracked and the pressure dropped indicating stress relaxation.

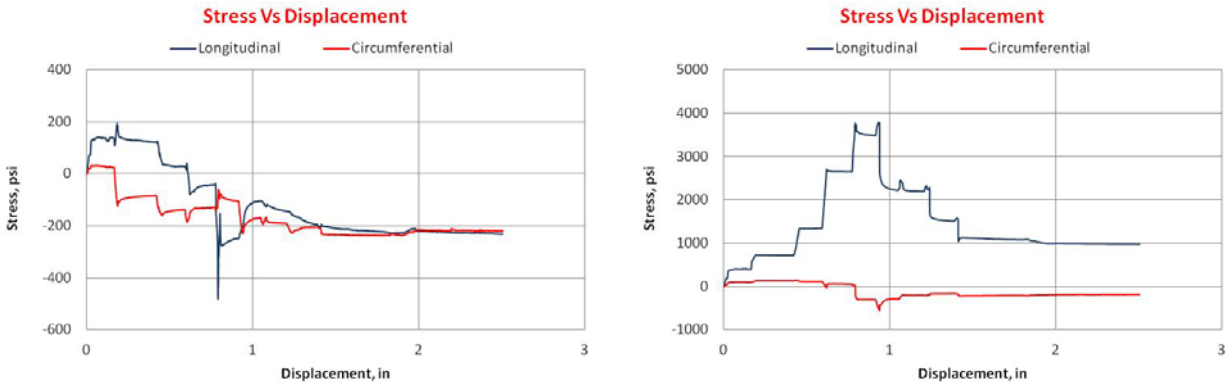

Figure 19: Response of strain rosettes at crown (left) and spring-line (at location of externally applied load; right)

As the displacement reached 1.5 in. the host-pipe cracked at the crown-invert plane and de-bonded from the liner. Following the failure of the host pipe, that liner was found to be able to hold 60 psi internal pressure. The liner ruptured at a lateral displacement of 3.5 in. and an internal pressure of 100 psi (see Figure 20).

Figure 20: Host-pipe broke at crown-invert plane (left) and 3.5 in. displacement of the liner (right)

5.2. NON-PRESSURIZED CONDITION

A schematic diagram of the experimental setup is shown in Figure 21. Specimen preparation and experimental setup were similar to these described in Section 5.1. Geometrical changes within the host pipe and the liner were observed as shear displacement increased from zero to approximately 4 in. The actuator was paused at increments of 0.25 in., and the host pipe and liner were inspected.

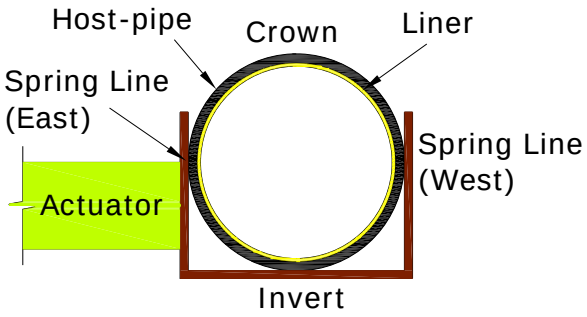

Figure 21: Schematic diagram of test specimen

Stain gauges were installed at the outer wall of the liner to obtain accurate strain measurements at the location of the ring break (see Figure 22).

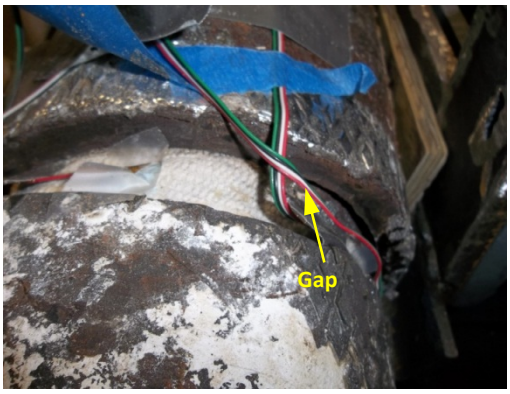

Figure 22: Strain gauge installed on the liner

The liner at the displaced section de-bonded from the host-pipe at the spring line (west) when the shear displacement reached about 2 in. As the specimen was not pressurized, the gap between the inner wall of the host pipe and the outer wall of the liner increased with the increasing displacement and propagated from the spring line region (west) to the invert area. Thus, relatively low stresses developed at the spring line (west) and invert. The liner exhibited a complete de-bonding from the pipe's wall at the spring-line (West) and invert, when the shear load reached around 7 kip at a displacement of 3.5 in. (see Figure 23).

Figure 23: Response of strain rosettes at spring-line (west) (left) and at invert (right)

Figure 24 depicts readings measured by the strain rosettes installed at the spring-line (West) and invert. The longitudinal stress at the spring line increased to around 900 psi as the liner stretched and elongated at the initiation of the applied external load. The ‘steps’ in the stress diagram indicate stress relaxation after each displacement increment. Compressive stresses in the circumferential direction of about 375 psi were measured at the invert. The data suggests that the liner elongated at the spring line while simultaneously compressed at the invert.

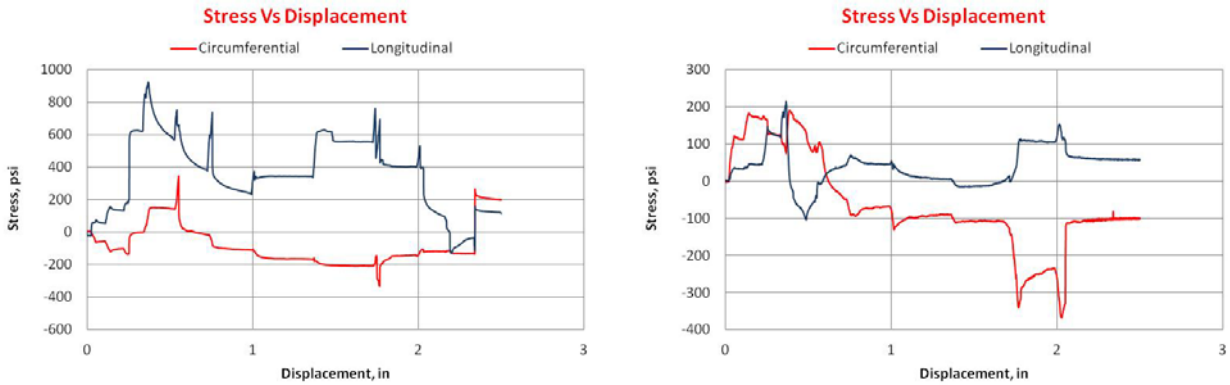

Figure 24: Response of strain rosettes at spring-line (west) (left) and at invert (right)

6. CONCLUSION

Results obtained from the physical testing of Aqua-Pipe®, a glass-fiber reinforced CIPP liner installed in a host pipe with a simulated ring fracture, were presented. It was concluded that the liner, subjected to internal pressure, was able to maintain its structural integrity even after the host-pipe failed. In one test, the deformed liner (vertical deflection = 5.0 in.) was subjected to an internal pressure of 120 psi for about one hour with no visible signs of leakage or structural distress. Under non- pressurized conditions, the liner buckled at the invert during the bending test and deformed sideways during the shear test, resulting in a reduction in the cross-sectional area at the location of the ring fracture. No change in the cross-sectional area was observed during the uni-axial tensile test.

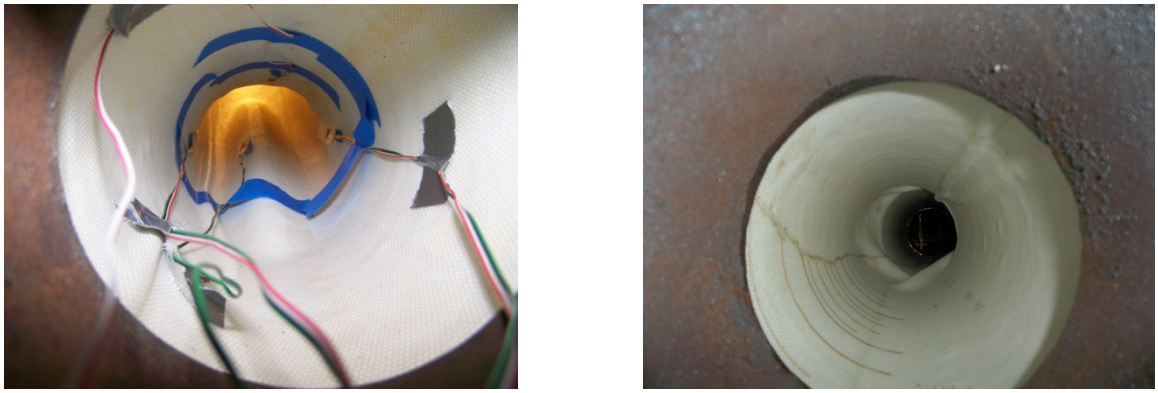

Figure 25: Formation of fold at the invert due to vertical displacement (left); lateral deformation of the liner caused by lateral displacement (right)

Aqua-Pipe® was found capable of sustaining high internal pressure well at locations of extreme angular deflection for at least short time periods, even after the host-pipe experienced complete failure. The liner was found to perform adequately, even after undergoing lateral deformation equal to 50% of the pipe's external diameter at the location of a ring fracture, potentially making it a suitable candidate for the lining of firefighting waterlines in areas prone to seismic activity. A high degree of friction was noted at the liner-host pipe interface during uni-axial test, as resin filled the corrosion pits in the inner wall of the host pipe resulting in a mechanical interlock equal to 1800 lbf per square foot of liner surface area.

7. REFERENCES

Alam, S., Allouche, E., Dulam, R. (2011). “Performance of Fiber-Reinforced CIPP Liner at the Location of Ring Fractures When Subjected to Angular Displacement.” *Proc. of Annual Technical Conference of the North American Society for Trenchless Technology*, Washington D.C.,581-589.

Allouche, E.N., Bainbridge, K., and Moore, I.D. (2005), “Laboratory examination of a cured-in-place pressure pipe liner for potable water distribution pipes.” *Proc. of Annual Technical Conference of the North American Society for Trenchless Technology* (CD ROM), Orlando, Florida, D-3-04.

ASTM F1216-07b: Standard Practice for Rehabilitation of Existing Pipelines and Conduits by the Inversion and Curing of a Resin-Impregnated Tube.

ASTM F1743: Standard Practice for Rehabilitation of Existing Pipelines and Conduits by Pulled-in-Place Installation of Cured-in-Place Thermosetting Resin Pipe (CIPP).

Brown, M., Fam, A., Moore, I.D. (2008). “Material characterization of components and assembled behavior of a composite liner for rehabilitation of cast iron pressure pipes.” *Polymer Engineering and Science*, 48(7), 1231-1239.

Zhao, D., Nassar, R., Hall, D. (2005), "Design and reliability of pipeline rehabilitation liners." *Tunneling and Underground Space Technology*, 20(2), 203-212.